



Photocatalytic degradation of rolling emulsion wastewater over titanium dioxide suspensions

Peng Jiang^a, Yun Li^a, Amanda Han^b, Xue-Qin Chen^a, Xiao-Long Zhou^{a,*}

^aInternational Joint Research Center of Green Chemical Engineering, Institute of Chemical Engineering, East China University of Science and Technology, Shanghai 200237, China, emails: xiaolong@ecust.edu.cn (X.-L. Zhou), 15216602608@163.com (P. Jiang), 625205857@qq.com (Y. Li), 18721322771@163.com (X.-Q. Chen)

^bEthoca Chemical INC., No.88 Feng Yang Road, Shanghai 200040, China, email: fang.han@ethocachemical.com (A. Han)

Received 27 December 2019; Accepted 6 May 2020

ABSTRACT

The rolling emulsion wastewater produced during steel production is harmful to the environment. Photocatalytic degradation over titanium dioxide (TiO₂) suspensions is employed to purify this wastewater under ultraviolet irradiation. The degradation of the pollutants in the wastewater is mainly attributed to photocatalysis and not photolysis. The impacts of the TiO₂ dosage and the pH on the degradation, as well as the concentration of dissolved oxygen (DO) on the retention time, are studied. Furthermore, the effect of agglomeration on the chemical oxygen demand (COD) removal efficiency is discussed. The distribution of photo-holes and the surface charge of TiO₂ change with the pH. The optimal parameters are as follows: a TiO₂ dosage of 4 g/L and an initial pH of 7.9. After 210 h of reaction under these conditions, the COD concentration decreases to 197.16 mg/L, and the wastewater after treated meet the indirect discharge standard. The duration of degradation can be shortened to 120 h by increasing the DO content to 10.75 mg/L in wastewater. In addition, the electrical energy consumption ($E_{EO} = 2.237 \times 10^3$ kW h/m³/order) for the photocatalytic degradation of rolling emulsion wastewater is provided.

Keywords: Photocatalysis; Wastewater; Titanium dioxide; COD; E_{EO}

1. Introduction

Rolling emulsion, which is widely used in steel production, commonly contains water, palm oil, surfactants, and other chemical additives. The disposal of waste emulsion, generated during the production process, is necessary to maintain the performance of the machine at a definite level after repeated use considering economic and environmental factors. If discharged directly, waste emulsion could threaten water security and human health, particularly because it is difficult to degrade naturally [1]. Generally, waste rolling emulsion is first pretreated by demulsification, after which the water phase of the rolling emulsion wastewater

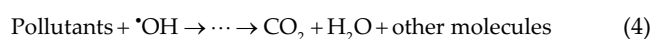
is purified to remove dissolved organic matter. Due to the presence of surfactants and various chemical additives, rolling emulsion wastewater has a complex composition and high chemical oxygen demand (COD, 3,000–4,000 mg/L), which makes it a pollutant in the environment. According to the effluent standard for the iron and steel industry in China, rolling emulsion wastewater is discharged into the public sewage system for further processing (indirect discharge) only if its COD concentration is less than 200 mg/L.

Nowadays, electrochemical oxidation, chemical oxidation, biological processes, and membrane filtration are widely investigated and developed for rolling emulsion

* Corresponding author.

wastewater disposal [1]. Although these methods have been proven to be effective, they still have some disadvantages. For instance, electrochemical oxidation can efficiently remove pollutants in sewage [2]; however, the electrodes are easily damaged during the treatment of high concentrations of rolling emulsion wastewater [3]. The Fenton process is a representative chemical oxidation method, which involves the catalytic decomposition of H_2O_2 by Fe^{2+} to form a hydroxyl radical, followed by the degradation of organic matter [4]. However, if the compositions of the wastewater are complicated, a large amount of hydrogen peroxide and acid will be consumed. Moreover, the transport or storage of these reagents and byproducts ($Fe(OH)_3$) restricts the application of the Fenton process to rolling emulsion wastewater disposal. Some pollutants in rolling emulsion wastewater, such as tetrahydroxymethyl phosphonium sulfate and Starcide BK, acting as bactericides, are difficult to be directly processed by a biochemical process. Membrane filtration is one of the methods that can intercept the organics by selective permeation [5]. However, a high concentration of pollutants easily plugs the membrane pore, which is expensive. In addition, oxidation processes based on persulfates have been developed for wastewater, but suitable strategies for activating persulfates are still being explored [6,7]. Therefore, it is necessary to develop a new alternative method, which has a high removal efficiency and environmentally friendly advantages.

Photocatalytic degradation is a rapidly expanding technology used for sewage disposal without secondary pollution. Under ultraviolet (UV) irradiation, some semiconductor materials can act as photocatalysts for heterogeneous degradation. These semiconductors have two separate bands: a valence band (VB) and a conduction band (CB) [8]. According to Eqs. (1)–(5), when the photon energy absorbed from light equals or exceeds the bandgap energy between the VB and CB, the catalyst would be excited to generate electron (e^-)/hole (h^+) pairs. The electrons have strong reducibility, and the holes have strong oxidizability. They will react with the matter adsorbed on the photocatalyst surface before recombination occurs to produce hydroxyl radicals ($\cdot OH$), which degrade the pollutants into CO_2 , H_2O , and some other molecules finally. The most used semiconductor as a photocatalyst is titanium dioxide (TiO_2). It has a suitable bandgap energy (3.0–3.2 eV) and can be excited by UV light with a wavelength below 387.5 nm. Furthermore, TiO_2 is inexpensive, non-toxic, and highly chemically stable (avoids photo-corrosion). These advantages make its utilization in practical wastewater purification normally possible [8].



In previous literature, the photocatalytic process is only widely used to decontaminate wastewater with low pollutant concentrations [9–11], or water would exhibit high turbidity, in which case the photocatalyst can be easily deactivated. Although the COD is as high as several thousands, rolling emulsion wastewater is transparent; thus, the excitation of TiO_2 will not be involved. In addition, it has been reported that spent TiO_2 can be easily regenerated by hydrogen peroxide treatment [12]. Therefore, the photocatalytic degradation of rolling emulsion wastewater is a possibility.

In this study, the photocatalytic degradation of rolling emulsion wastewater over TiO_2 suspensions is investigated. The effects of the TiO_2 dosage and the pH on the COD removal efficiency are studied. Additionally, the effect of the dissolved oxygen (DO) concentration on the degradation time is investigated. Mechanisms are discussed based on experimental results and characterization. The electrical energy consumption (E_{EO}) is also calculated to evaluate the economic viability of the process.

2. Materials and methods

2.1. Chemicals

The rolling emulsion wastewater was sourced from Xiehe steel rolling factory in Jiangsu, China. Nano- TiO_2 (P25) was provided by Degussa (Germany), and the average particle size was 20 nm. The chemicals, H_2SO_4 (98%), NaOH (AR), $K_2Cr_2O_4$ (AR), $(NH_4)_2Fe(SO_4)_2 \cdot 6H_2O$ (AR), and $AgSO_4$ (AR), were all obtained from Taitan Co. All solutions were prepared with distilled water.

2.2. Wastewater characterization and analytical methods

The properties of rolling emulsion wastewater are shown in Table 1. The pH was measured using a pH meter (INESA PHSJ-4). The COD concentrations were measured using the potassium dichromate oxidation method, which is in line with ASTM D1252-06. Ion chromatography (ICS-1100) was used to obtain the concentration of inorganic anions. An ultraviolet illuminometer (Lutron TN2254) was used to determine the light intensity. The DO content in wastewater was analyzed using a DO analyzer (Hach HQ30D). The average particle sizes of the photocatalyst before and after the reaction were measured using a laser scattering particle-size and shape analyzer (Microtrac S3500SI). The surface potential of the nano TiO_2 particles was determined using the ZETA potential analyzer (Zetasizer Nano ZS). The catalyst was also characterized using a Fourier-transform infrared spectrometer (FTIR, Nicolet 6700) in the wavenumber range of 400–4,000 cm^{-1} . The carbon content was measured using an elemental analyzer (Elementar Vario ELIII).

2.3. Experimental setup and procedure

The experimental setup is shown in Fig. 1. The main reactor is a 0.5 L cylindrical quartz photoreactor. It is connected to a 0.5 L three-necked flask by a silicone tube. The wastewater in the flask is introduced from the bottom of the reactor by a peristaltic pump at a rate of 0.11 L/min to receive UV irradiation. Magnetic stirrers are used to maintain

a uniform distribution of TiO_2 in the reactor. A 15 W UV lamp with typical λ of 254 nm and intensity of 2.0 mW/cm^2 is placed in the middle of the reactor to provide energy.

The experiment is carried out at 25°C. Wastewater is mixed with the TiO_2 particles for 1 h in a dark environment until adsorption equilibrium is achieved under the mixing conditions. The sample is collected periodically using a microsyringe and subsequently filtered using a 0.22 μm polyethersulfone membrane to remove the solid catalyst.

The effect of the preparation parameters on the degradation behaviors was examined by varying the TiO_2 dosage between 0, 2, 4, 6, 8, and 10 g/L, and the initial pH between 2.0, 5.5, 7.9, and 10.0, respectively. H_2SO_4 and NaOH were used to adjust the solution pH. Moreover, the DO content was regulated by aerating nitrogen, air, and oxygen into the wastewater.

The reaction rate (r , $\text{mg}/\text{L}/\text{h}$) was calculated according to Eq. (6):

$$r = -\frac{dC}{dt}, \quad (6)$$

where C is the pollutant concentration (COD) in mg/L , and t is the retention time in h.

The COD reducing efficiency (η , %) was defined by:

Table 1
Properties of the rolling emulsion wastewater

Property	Value
pH	7.9
COD (mg/L)	3,573
Cl^- (mg/L)	717
Ca^{2+} (mg/L)	137
NH_4^+ (mg/L)	48

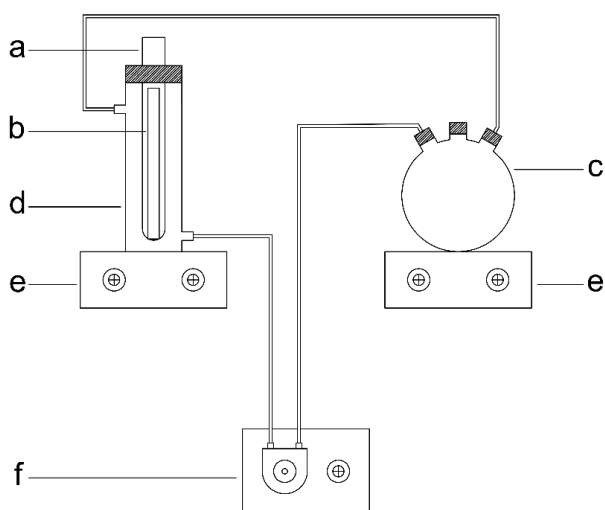


Fig. 1. Experimental setup: (a) quartz tube, (b) UV lamp, (c) three-necked flask, (d) photoreactor, (e) magnetic stirrer, and (f) peristaltic pump.

$$\eta = \frac{C_0 - C_f}{C_0} \times 100\% \quad (7)$$

where C_0 and C_f are the initial and final pollutant concentrations (COD) in mg/L .

3. Results and discussion

3.1. Photolysis vs. photocatalysis

A comparative study is carried out to determine the effect of photolysis, which is shown in Fig. 2.

It is observed that the pollutant concentration in the wastewater containing 2 g/L of TiO_2 gradually decreases upon irradiation. The degree of COD removal reaches 25.71% and almost remains unchanged for 40 h on stream. Conversely, the COD removal only reaches 6.46% at the same time on stream without the photocatalyst in the reactor. These results demonstrate that only a few organic matters in wastewater are removed by self-photolysis, and pollutant degradation is mainly attributed to photocatalysis.

3.2. Effect of the TiO_2 dosage

To examine the effect of the catalyst dosage, the pollutant concentrations are measured at five different TiO_2 dosages. As shown in Fig. 3, the degree of COD removal is improved when the TiO_2 dosage is increased from 2 to 4 g/L, resulting from the gradual degradation of initial organic compounds to various intermediate products. This can be explained by the presence of more active sites for adsorption and degradation. However, the removal degree reaches a maximum at 4 g/L, after which a decrease is observed upon further increase of the photocatalyst dosage. Similar results for UV/ TiO_2 photocatalytic degradation have also been reported in previous works [13,14]. These results are observed firstly because nano- TiO_2 is prone to agglomeration in wastewater by chemical forces, which can

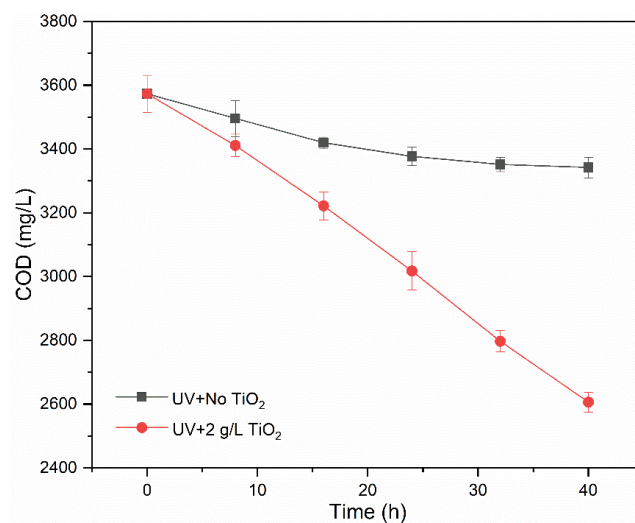


Fig. 2. Extent of photolytic and photocatalytic degradations of the pollutant.

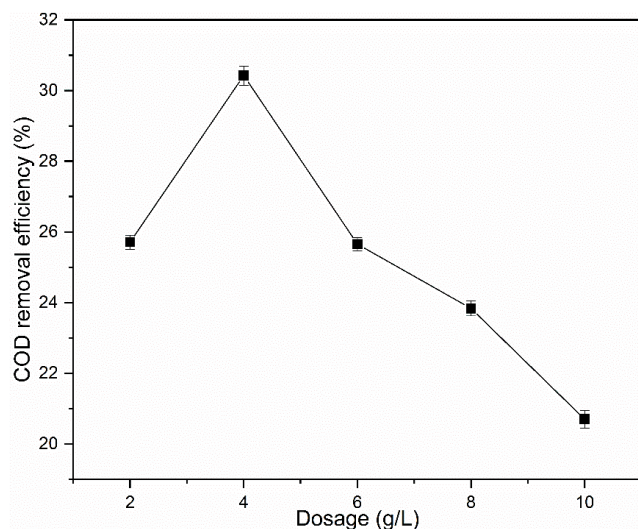


Fig. 3. Variation of the COD removal efficiency with different TiO_2 dosages.

be observed by particle-size analysis. Secondly, the intermediate product adsorption also aggravates the interaction.

As shown in Table 2, the TiO_2 particles grow from 20 nm to $\sim 4 \mu\text{m}$ after the reaction. Since the average sizes are much larger than the wavelength of incident light (254 nm), the micron-sized particles lose the ability to scatter incident light. The particles, closer to the light source, will mainly reflect the light and assist those located farther to receive UV light, as shown in Fig. 4. The dosage is proportional to the number of micron-sized particles in the wastewater; the reflection is more marked as the catalyst dosage increases. These results can be demonstrated by measuring the residual light intensity after UV light passes through the wastewater. The results of this measurement are listed in Table 3, and it is demonstrated that the higher the catalyst concentration, the lower the residual light intensity. The full utilization of the UV source is difficult under this condition.

The photocatalyst has two opposite effects on the degradation process. Subsequently, based on the discussion above, a photocatalyst dosage of 4 g/L is used to evaluate the effect of other parameters on the photocatalytic degradation of rolling emulsion wastewater.

3.3. Effect of pH

The pH is one of the most important parameters in this process. The photocatalytic degradation efficiency is measured at three different initial pH values of wastewater, as given in Fig. 5. It can be observed that the lowest degradation appears at an initial pH of 2.0. The efficiency increases with the pH until the maximum value is reached at a pH of 7.9, which is considered as the optimal pH required for effective degradation in this work.

The variations of the pH and reaction rates are presented in Figs. 6 and 7, respectively. As shown, the pH of the wastewater continually decreases during the reaction. It has been reported in previous literature that some acidic

Table 2
Average particle size of TiO_2 obtained after 40 h of reaction

Dosage (g/L)	Particle size (μm)
2	4.89
4	4.92
6	4.01
8	4.44
10	4.23

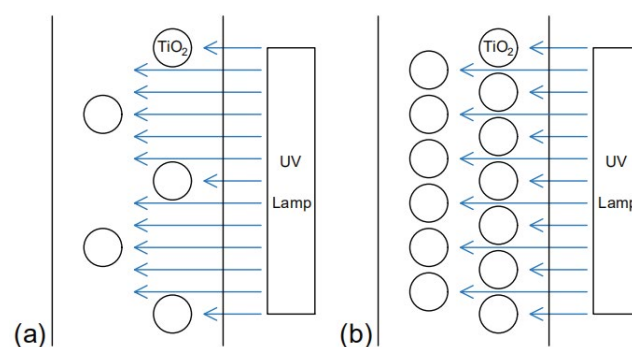


Fig. 4. UV light irradiation of wastewater with different TiO_2 dosages: (a) low dosage and (b) high dosage.

Table 3
Residual light intensity after UV light passes through the wastewater

Catalyst dosage (g/L)	Light intensity ($\mu\text{W}/\text{cm}^2$)
0	35.2
2	1.5
4	1.2
6	1.0
8	0.8
10	0.5

intermediates, such as formic acid and acetic acid, can be produced during the degradation process [12,14]. The pH decline is caused by the deprotonation of the intermediates. Further, as the pH decreases, the reaction rate profiles for all runs at pH values higher than 2.0 reach the maximum.

The effect of pH on the heterogeneous photocatalytic degradation is mainly explained in two aspects: the distribution of photo-holes and the surface charge of nano- TiO_2 particles.

The effect of pH on the distribution of photo-holes can be described as follows. The reaction that occurs at the interface between TiO_2 (an *n*-type semiconductor in this study) and wastewater is beneficial to the degradation, as can be seen in Eq. (2). As shown in Fig. 8a, the standard redox potential of $\cdot\text{OH}/\text{H}_2\text{O}$ is about 2.68 V vs. NHE [15], which lies between the VB potential (E_{VB} , 3.08 V vs. NHE) and CB potential (E_{CB} , -0.12 V vs. NHE) of the catalyst, and is higher

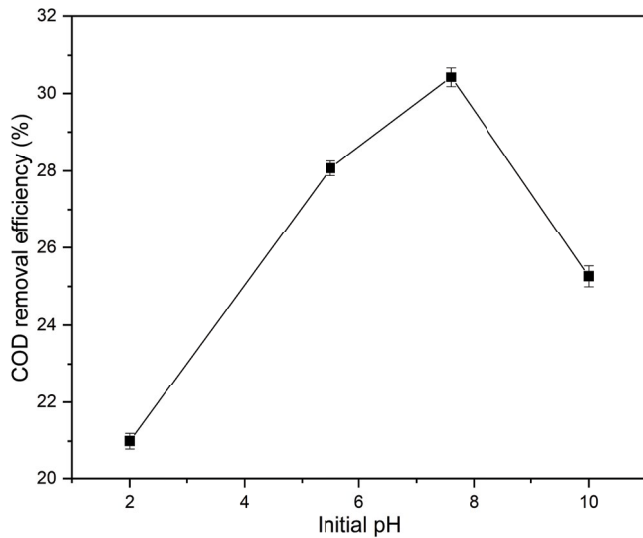


Fig. 5. Variation of the COD removal efficiency with different initial pH values.

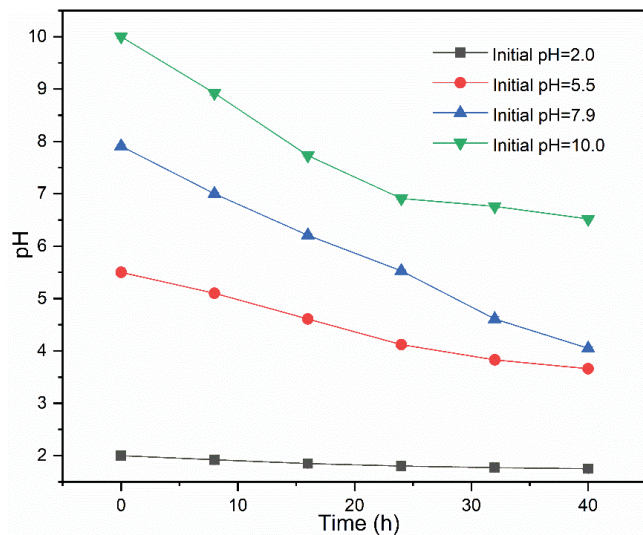


Fig. 6. Variation of the wastewater pH with time.

than the Fermi energy potential (E_{FV} is close to E_{CB} in an n -type semiconductor).

Photo-electrons are transferred to the side close to the wastewater, driven by the potential difference; they migrate from a space charge region with a relatively high concentration of photo-holes at the side of the TiO_2 to produce $\cdot OH$ [16]. The redox potential of $\cdot OH/H_2O$ ($E_{(\cdot OH/H_2O)}$, V vs. NHE) varies with the pH of wastewater and can be calculated by the Nernst relationship shown in Eq. (8):

$$E(\cdot OH/H_2O) = 2.68 - 0.059 \times pH \quad (8)$$

When the pH decreases, the value of $E_{(\cdot OH/H_2O)}$ increases, as shown in Fig. 8b, and the potential difference increases also. As a result, the concentration of photo-holes in the space charge region increases. This is beneficial for the

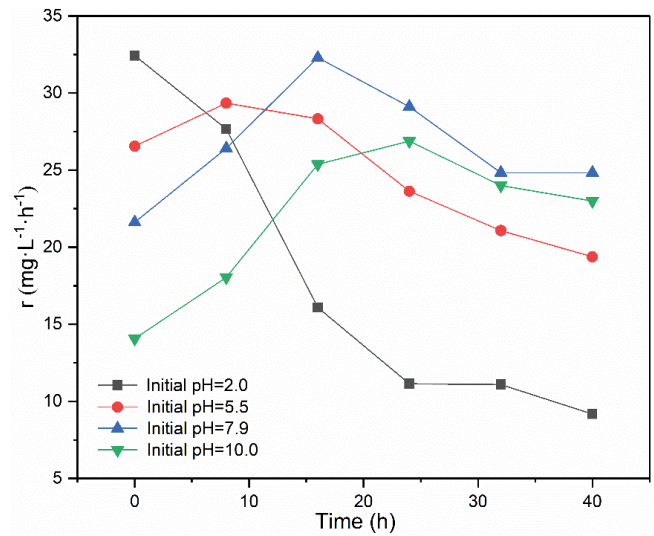


Fig. 7. Variation of the reaction rates with different initial pH values.

generation of $\cdot OH$, which consequently improves the degradation rate of wastewater.

Meanwhile, the surface charge of TiO_2 can be influenced by the pH according to the analysis of the Zeta potential demonstrated in Fig. 9. The zero point of charge (pH_{zpc}) of nano- TiO_2 used in the study is equal to 6.7. When the pH is lower than 6.7, particles are protonated, as expressed in Eq. (9), and a positive charge appears at the surface of TiO_2 . The negative ions generated by the dissociation of acidic intermediates can be easily adsorbed on the surface of the catalyst through electrostatic attraction, resulting in a decrease in the number of active sites and reaction rates. Conversely, when the pH is greater than 6.7, the surface charge of the catalyst is negative, according to Eq. (10). Negative anions are repulsed by the catalyst particles, and the surface charge is not the dominant factor under this condition.



The amount of intermediates produced by the reaction is less at the beginning of the reaction; the effect of the photo-hole distribution on the COD removal rates is more significant than that of the surface charge. As shown in Fig. 7, the initial reaction rates decrease with the initial pH, from 2.0 to 10.0. This is caused by the decrease in the concentration of photo-holes in the space charge region. As the reaction progresses, more intermediates are produced, leading to a decrease in the pH. Consequently, the concentration of photo-holes increases gradually, and the reaction rates reach a maximum, except for the group at the initial pH of 2.0.

Comparing with Figs. 6 and 7, it can be observed that when the initial pH is 7.9 or 10.0, the pH values of the wastewater reduce to around 6.7 (pH_{zpc}) at the same time as the rates rise to the maximum. With further degradation, many

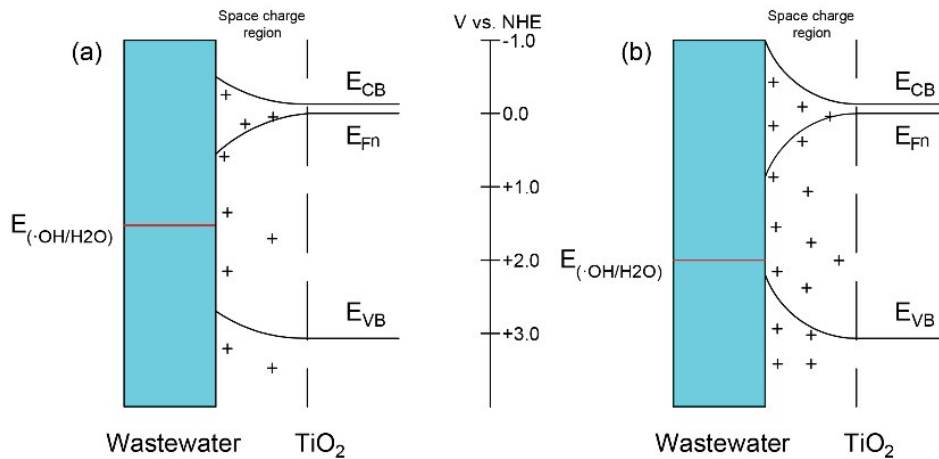


Fig. 8. Energy-band diagram of wastewater and TiO₂ contact: (a) high pH and (b) low pH.

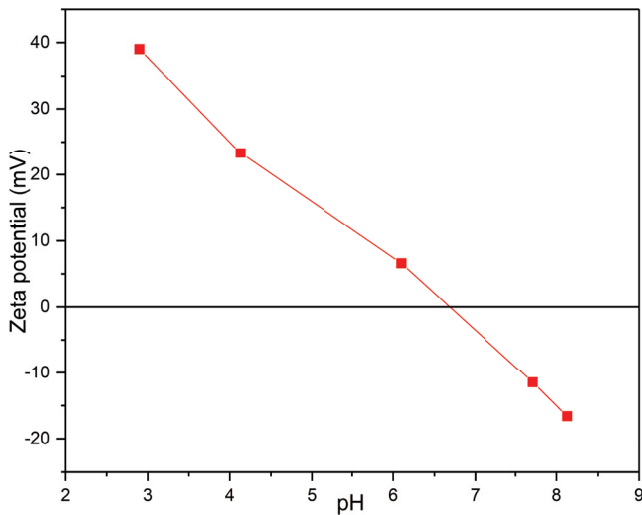


Fig. 9. Variation of the Zeta potential of fresh nano-TiO₂ with different pH values.

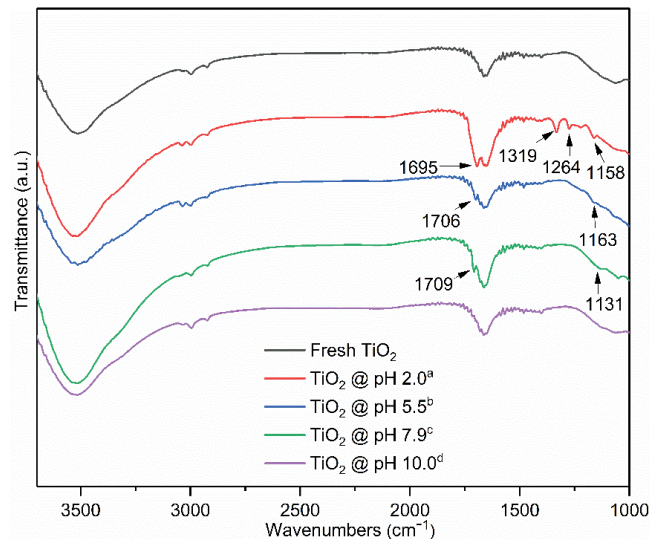


Fig. 10. FTIR spectra of TiO₂ obtained before and after 40 h of reaction.

intermediates are produced, leading to a further decrease in the pH of the suspension. Consequently, the surface charge of the catalyst particles would be positive. At this time, the effect of pH on the surface charge gradually becomes dominant in the reaction. Negative ions can be adsorbed on the surface of TiO₂, resulting in a decrease in the reaction rates. Since it is unavoidable, a trend similar to that of the rates is found in the group with an initial pH of 5.5. The effect of pH on the surface charge is significant at an initial pH of 2.0, resulting in a continuous decline in the rates from the beginning of the degradation.

The adsorption of intermediates can be proven by FTIR spectroscopy and carbon content measurement of TiO₂ obtained after 40 h of reaction. As shown in Fig. 10, all the IR spectra possess two characteristic peaks at 1,626 and 3,421 cm⁻¹, attributed to the hydroxyl groups. In the FTIR spectra of TiO₂, obtained at the initial pH of 2.0, four absorption peaks at 1,158; 1,264; 1,319; and 1,695 cm⁻¹ can be observed. The spectra of TiO₂ in the group of initial pH 5.5

have two peaks at 1,163 and 1,706 cm⁻¹. Similarly, the spectra of TiO₂ in the group of initial pH 7.9 have two peaks, located at 1,131 and 1,709 cm⁻¹, respectively.

The bands at 1,695; 1,706; and 1,709 cm⁻¹ are attributed to the >C=O bonds of the carboxylate groups (-COO⁻), while the peak at 1,319 cm⁻¹ belongs to the -C-O- bonds of -COO⁻. All these results indicate that the acidic organic components are adsorbed on the surface of TiO₂. In addition, the bands at 1,131; 1,158; 1,163; and 1,264 cm⁻¹ are attributed to the C-O-C bonds, which are formed by the outer sphere complexation of the -COO⁻ groups of the adsorbed matters on the catalyst surface [12]. As the initial pH increases, the number of absorption peaks, resulting from the intermediates, gradually decreases. No notable additional absorption peaks can be observed in the group of initial pH 10.0.

The carbon content of TiO₂ is shown in Table 4, wherein the carbon content reduces as the initial pH increases, reaching a minimum of 0.19%, which is obtained at an initial

Table 4
Carbon content of TiO₂ obtained before and after 40 h of reaction

Catalyst	Carbon content (wt.%)
Fresh TiO ₂	Nil
TiO ₂ at pH 2.0	1.64
TiO ₂ at pH 5.5	1.01
TiO ₂ at pH 7.9	0.84
TiO ₂ at pH 10.0	0.19

pH of 10.0. This result explains why there are no distinct absorption peaks in the spectrum of pH 10.0. The data of the carbon content is in line with the FTIR analysis results.

3.4. Effect of DO on the degradation time

According to the discussion above, the COD in the rolling emulsion wastewater can be degraded to a final concentration of 197.16 mg/L with a TiO₂ dosage of 4 g/L and an initial pH of 7.9 after 210 h. The wastewater after treatment is able to meet the indirect discharge standard after the treatment and can be discharged into the public sewage system for further processing. However, the duration of degradation is overly long for practical use.

To confirm if increasing the DO content can shorten the time, different gases are introduced into the wastewater. The results are shown in Figs. 11 and 12, wherein the original DO content in the wastewater is 7.34 mg/L.

When nitrogen is aerated into the water, the concentration of oxygen drastically drops to 1.52 mg/L; consequently, the photocatalyst exhibits no significant activity. As the concentration of DO increases, the rates of degradation also increase. After 120 h, the residual value of COD (196.25 mg/L) reduces to a final level similar to that without aeration, while other gases are replaced by oxygen. The duration of degradation is, therefore, shortened to about half of 210 h.

The weakly effective utilization of photo-holes has always restricted the heterogeneous photocatalytic degradation efficiency. Electron-hole pairs lose their effects after recombination [8]. Therefore, this process should be inhibited to enhance degradation efficiency.

As shown in Eq. (3), oxygen in water usually plays the role of an electron acceptor. Since this reaction can delay the recombination of electron-hole pairs, the degradation can be accelerated by increasing the concentration of DO in wastewater.

3.5. Electrical energy consumption for the photocatalytic degradation of rolling emulsion wastewater

For practical use, it is necessary to evaluate the economic viability of this process. The electrical energy per order (E_{EO}) is an important figure-of-merit in advanced oxidation processes (AOPs) for the use of electrical energy, and it has been accepted by the International Union of Pure and Applied Chemistry (IUPAC) [17]. It is defined as the amount of electrical energy in kilowatt-hours required to reduce the concentration of organic matters by one order

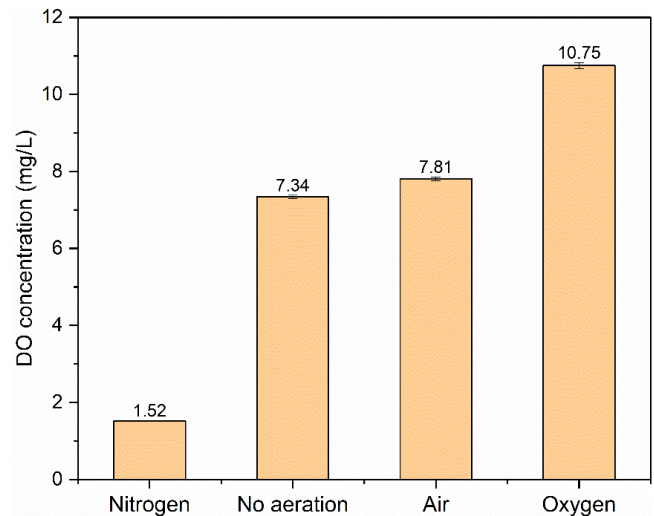


Fig. 11. Variation of the DO concentration in wastewater with different gases.

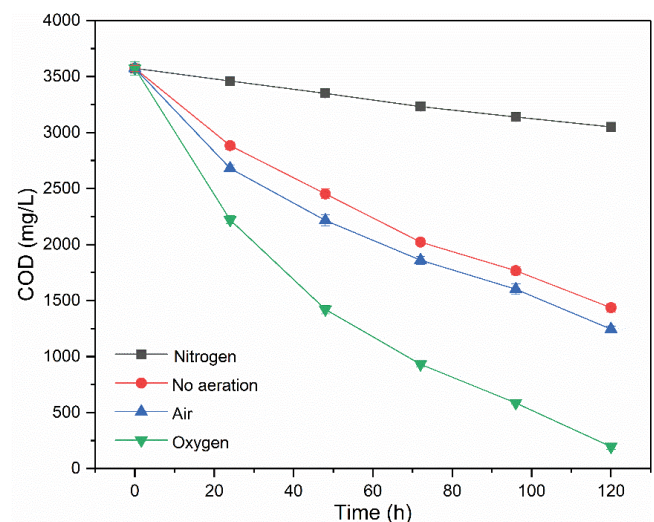


Fig. 12. Variation of the COD value with different gases.

of magnitude in a unit volume of wastewater. The method of obtaining a low E_{EO} is highly efficient. The photocatalytic degradation of palm oil emulsion wastewater has been analyzed using the pseudo-first-order kinetic model [18]. For this study, E_{EO} (kW h/m³/order) is calculated using the following equation:

$$E_{EO} = \frac{P \times t \times 1,000}{V \times \lg(C_0/C_f)} \quad (11)$$

$$\ln\left(\frac{C_0}{C_f}\right) = k \times t, \quad (12)$$

where P (kW) is the power of the UV lamp used for the degradation. t (h) is the duration of the operation. V (L) is the volume of the wastewater sample in the experiment. A factor

of 1,000 is used to convert L to m³. C_0 and C_f are the initial and final pollutant concentrations (COD) in mg/L, and k is the pseudo-first-order rate constant (h⁻¹) of the degradation.

The volume, V , of the wastewater sample used here, is 0.8 L, and the power, P , is 15 W. Therefore, Eq. (11) can be reduced to:

$$E_{EO} = \frac{15}{0.3474k} \quad (13)$$

Under the optimal conditions, including a TiO₂ dosage of 4 g/L, pH of 7.9, and DO concentration of 10.75 mg/L, the rate constant, k , is 0.0193 h⁻¹ ($R^2 = 0.9963$). Therefore, the calculated value of E_{EO} for this process is 2.237×10^3 kW h/m³/order.

Ahaji et al. [18] and Ng et al. [19] utilized UV/TiO₂ process to degrade palm oil emulsion wastewater. The initial pollutant concentrations of their research are 350 and 170 mg/L, which are lower than our work. However, higher E_{EO} values of 3.217×10^3 and 6.962×10^3 (calculated according to experimental data) kW h/m³/order were obtained. The comparison shows that rolling emulsion wastewater can be treated effectively in our study.

4. Conclusions

Rolling emulsion wastewater can be purified by photocatalytic degradation over TiO₂ suspensions. The degradation is exclusively attributed to photocatalysis and not photolysis. The optimal conditions are as follows: TiO₂ dosage of 4 g/L, initial pH of 7.9, and DO concentration of 10.75 mg/L. After the treatment under the optimal conditions, the wastewater could meet the indirect discharge standard. The degree of removal gradually increases with the dosage of the photocatalyst, although the irradiation of UV light is weakened by the agglomeration caused by an excess amount of catalysts. Since the relative concentration of photo-holes in the space charge region is inversely proportional to the pH, high reaction rates are obtained at low pH values. However, a positive charge is formed on the catalyst surface when the pH is lower than 6.7 (pH_{zpc}). This results in a decrease in both the number of active sites and the reaction rates by adsorption of negative ions. Oxygen in water usually plays the role of an electron acceptor to inhibit the recombination of electron-hole pairs. The figure-of-merit E_{EO} meets the requirement, and our study shows that rolling emulsion wastewater can be treated effectively with the UV/TiO₂ process with an E_{EO} value of 2.237×10^3 kW h/m³/order.

Acknowledgments

This research did not receive any specific grant from funding agencies in the public, commercial, or not-for-profit sectors.

Symbols

E_{EO} — Electrical energy per order, kW h/m³/order
 r — Reaction rate, mg/L/h
 C_0 — Initial concentration of pollutants (COD), mg/L

C_f — Final concentration of pollutants (COD), mg/L
 t — Retention time, h
 η — COD reducing efficiency, %
 E_{VB} — Valence band potential, V
 E_{CB} — Conduction band potential, V
 E_{Fn} — Fermi energy potential, V
 $E_{(OH/H_2O)}$ — Redox potential of [•]OH/H₂O, V
 P — Power of UV lamp, kW
 V — Volume, L
 k — Pseudo first-order rate constant, h⁻¹

Supplementary data

Electronic Supplementary Material associated with this article can be found in the online version of this paper (DOI: 10.17632/xwgd34nf8.2).

References

- [1] Y. Zhang, F. Gan, M. Li, J. Li, S. Li, S. Wu, New integrated processes for treating cold-rolling mill emulsion wastewater, *J. Iron Steel Res. Int.*, 17 (2010) 32–35.
- [2] F. Moreiraa, R. Boaventuraa, E. Brillasb, V. Vilara, Electrochemical advanced oxidation processes: a review on their application to synthetic and rolling wastewaters, *Appl. Catal., B*, 202 (2017) 217–261.
- [3] S. Garcia-Segura, J. Ocon, M. Chong, Electrochemical oxidation remediation of rolling wastewater effluents – a review, *Process Saf. Environ. Prot.*, 113 (2018) 48–67.
- [4] V. Orescanin, R. Kollar, K. Nad, I.L. Mikelic, S.F. Gustek, Treatment of winery wastewater by electrochemical methods and advanced oxidation processes, *J. Environ. Sci. Health., Part A*, 48 (2013) 1543–1547.
- [5] G. Yi, X. Fan, X. Quan, S. Chen, H. Yu, Comparison of CNT-PVA membrane and commercial polymeric membranes in treatment of emulsified oily wastewater, *Front. Environ. Sci. Eng.*, 13 (2019) 261–280.
- [6] P. Shao, J. Tian, F. Yang, X. Duan, S. Gao, W. Shi, X. Luo, F. Cui, S. Luo, S. Wang, Identification and regulation of active sites on nanodiamonds: establishing a highly efficient catalytic system for oxidation of organic contaminants, *Adv. Funct. Mater.*, 28 (2018) 1705295.
- [7] P. Shao, X. Duan, J. Xu, J. Tian, W. Shi, S. Gao, M. Xu, F. Cui, S. Wang, Heterogeneous activation of peroxymonosulfate by amorphous boron for degradation of bisphenol S, *J. Hazard. Mater.*, 322 (2017) 532–539.
- [8] H. Zangeneh, A.A.L. Zinatizadeh, M. Habibi, M. Akia, M. Hasnain Isa, Photocatalytic oxidation of organic dyes and pollutants in wastewater using different modified titanium dioxides: a comparative review, *J. Ind. Eng. Chem.*, 26 (2015) 1–36.
- [9] S. Mahmoud, M. Mohamed, E. Hisham Kh, Synthesized nano titanium for methylene blue removal under various operational conditions, *Desal. Water Treat.*, 165 (2019) 374–381.
- [10] W. Khana, I. Najeebb, M. Tuiyebayevaa, Z. Makhtayevaa, Refinery wastewater degradation with titanium dioxide, zinc oxide, and hydrogen peroxide in a photocatalytic reactor, *Process Saf. Environ. Prot.*, 94 (2015) 479–486.
- [11] I.J. Ani, U.G. Akpan, M.A. Olutoye, B.H. Hameed, Photocatalytic degradation of pollutants in petroleum refinery wastewater by TiO₂- and ZnO-based photocatalysts: recent development, *J. Cleaner Prod.*, 205 (2018) 930–954.
- [12] V. Gandhi, M.K. Mishra, P. Joshi, A study on deactivation and regeneration of titanium dioxide during photocatalytic degradation of phthalic acid, *J. Ind. Eng. Chem.*, 18 (2012) 1902–1907.
- [13] R. Wu, C. Chen, C. Lu, P. Hsu, M. Chen, Phorate degradation by TiO₂ photocatalysis: parameter and reaction pathway investigations, *Desalination*, 250 (2010) 869–875.

- [14] M. Sanchez, M.J. Rivero, I. Ortiz, Photocatalytic oxidation of grey water over titanium dioxide suspensions, *Desalination*, 262 (2010) 141–146.
- [15] Y. Yao, G. Wu, F. Lu, S. Wang, Y. Hu, J. Zhang, W. Huang, F. Wei, Enhanced photo-Fenton-like process over Z-scheme $\text{CoFe}_2\text{O}_4/\text{g-C}_3\text{N}_4$ Heterostructures under natural indoor light, *Environ. Sci. Pollut. Res. Int.*, 23 (2016) 21833–21845.
- [16] M. Walter, E. Warren, J. McKone, S. Boettcher, Q. Mi, E. Santori, N. Lewis, Solar water splitting cells, *Chem. Rev.*, 110 (2010) 6446–6473.
- [17] R. Wu, C. Chen, M. Chen, C. Lu, Titanium dioxide-mediated heterogeneous photocatalytic degradation of terbufos: parameter study and reaction pathways, *J. Hazard. Mater.*, 162 (2009) 945–953.
- [18] M.H. Alhaji, K. Sanaullah, S.F. Salleh, R. Bains, S.F. Lim, A.R.H. Rigit, K.A.M. Said, A. Khana, Photo-oxidation of pre-treated palm oil mill effluent using cylindrical column immobilized photoreactor, *Process Saf. Environ. Prot.*, 117 (2018) 180–189.
- [19] K.H. Ng, M.M.R. Khan, Y.H. Ng, S.K.S. Hossain, C.K. Cheng, Restoration of liquid effluent from oil palm agroindustry in Malaysia using UV/TiO₂ and UV/ZnO photocatalytic systems: a comparative study, *J. Environ. Manage.*, 196 (2017) 674–680.